Lin et al. Nanoscale Research Letters (2015) 10:71
DOI 10.1186/s11671-015-0782-x

Nanoscale Research Letters
a SpringerOpen Journal

NANO EXPRESS Open Access

Pure electron-electron dephasing in percolative aluminum ultrathin film grown by molecular beam epitaxy

Shih-Wei Lin[1], Yue-Han Wu[2], Li Chang[2], Chi-Te Liang[3,4] and Sheng-Di Lin[1*]

Abstract

We have successfully grown ultrathin continuous aluminum film by molecular beam epitaxy. This percolative aluminum film is single crystalline and strain free as characterized by transmission electron microscopy and atomic force microscopy. The weak anti-localization effect is observed in the temperature range of 1.4 to 10 K with this sample, and it reveals that, for the first time, the dephasing is purely caused by electron-electron inelastic scattering in aluminum.

Keywords: Weak anti-localization; Ultrathin metal films; Pure electron-electron dephasing

Background

Weak localization (WL) is the quantum correction to the conductance which occurs in weakly disordered systems due to coherent backscattering of electrons (or holes). As a results of spin-orbit coupling, weak anti-localization (WAL) may be observed in a weakly disordered electron (or hole) system [1]. The theoretic derivation and experimental proof of WAL were extensively developed since 1980s, and the investigation on various materials in all dimensions has been a central topic in condensed matter physics for decades. In particular, a wide variety of experimental results of WAL were obtained in two-dimensional (2D) systems. 2D system is suitable for experimental study of WAL because of its stronger WAL contribution than three-dimensional (3D) ones and its easier sample fabrication than one-dimensional (1D) ones. Recently, due to its sensitivity to the electron dephasing and spin dephasing, WAL has been widely applied to studying the spin-orbit interaction in new materials, such as graphene, topological insulator, magnetic-doped semiconductor, and narrow-gap semiconductor, to evaluate the potential for spintronics devices [2-7].

In addition, the interplay between superconducting effect and WAL also attracts much attention and has been investigated extensively. Ebisawa et al. derived the relationship between the superconducting pair-breaking parameter δ and the inelastic scattering rate τ_i^{-1} by $\delta = (\pi\hbar/8k_BT)\tau_i^{-1}$ [8]. Their results have been used to study experiments of WAL in aluminum thin films [9-11]. However, it is a chanting challenge to grow an ideal 2D superconducting metallic sample. As the thickness of evaporated metal goes thinner, the discontinuity of the metal film un-avoidably appears due to large lattice mismatch between the template and metallic material as well as the surface non-uniformity of the bottom template. Previously, the reported metallic films were in the thickness of ten to a few tens of nanometers [9-14]. Although plenty of the theoretic works of WAL in two-dimensional systems have been published in the past few decades, the experimental proof toward WAL in an ideal two-dimensional metallic system is still lacking. In this work, we have used molecular beam epitaxy (MBE) system as the deposition technique to prepare ultrathin Al films. By using gallium-rich GaAs as the epi-template, we are able to successfully deposit ultrathin percolated Al film for studying WAL toward the 2D limit. Interestingly, we have observed a pure electron-electron dephasing in this sample over the whole temperature range that WAL effect exists. Note that all of our characterizations including structural and electrical assessments

* Correspondence: sdlin@mail.nctu.edu.tw
[1]Department of Electronics Engineering, National Chiao Tung University, 1001 University Road, Hsinchu 30010, Taiwan
Full list of author information is available at the end of the article

were fulfilled *ex situ*, and the continuity of the Al film remains even after the post-processing for the Hall device fabrication. Even though our sample is not thin enough to reach the ultimate two-dimensional limit such as monolayer graphene, our results still provide an experimental proof that Nyquist scattering becomes the dominant inelastic scattering mechanism at all temperatures when the system approaches an ideal two-dimensional one.

Theory

Magneto-resistance measurements are commonly used to study WAL. The theoretical calculation of 2D WAL in a perpendicular magnetic field was derived by Hikami, Larkin, and Nagaoka [1]. The difference of conductance induced by applied magnetic field can be expressed as:

$$\Delta g_{\mathrm{WAL}} = g(B) - g(0) = \frac{e^2}{\pi h}\left[\frac{3}{2}Y\left(\frac{B_2}{B}\right) - \frac{1}{2}Y\left(\frac{B_{\mathrm{i}}}{B}\right)\right]. \quad (1)$$

where B is the applied magnetic field. $Y(x)$ represents $\Psi(1/2 + x) - \ln(x)$, $B_2 = B_{\mathrm{i}} + 3/4B_{\mathrm{so}}$, $\Psi(x)$ is the digamma function. Here, B_{i} and B_{so} represent the strength of electron dephasing and spin-orbit interaction, respectively. For a superconducting material near its critical temperature T_c, superconducting fluctuations must be considered. Maki has calculated the effect of superconducting fluctuations in a 2D system (Δg_{MT}) [15]. Later, Thompson has modified the model by introducing the superconductor pair-breaking parameter δ to avoid the unphysical divergence at temperature near T_{c} [16]. The Maki-Thompson correction term was modified by Abrahams et al. that can be applied to higher field [17]:

$$\Delta g_{\mathrm{MT}} = -\beta\frac{e^2}{\pi h}\left[Y\left(\frac{B_{\mathrm{i}}}{B}\right) - Y\left(\frac{B_{\mathrm{T}}}{B}\right)\right], \quad (2)$$

where β represents the interaction strength between the electron pair [18]. Accordingly, $\beta \sim 1/[\ln(T/T_{\mathrm{c}}) - \delta]$ at temperature close to T_{c} [17]. $B_{\mathrm{T}} = 2k_{\mathrm{B}}T\ln(T/T_{\mathrm{c}})/\pi De$ and D is the diffusion coefficient, $D = 1/3v_{\mathrm{F}}l_0$. Here, v_{F} is the Fermi velocity and l_0 is the mean free path.

Bergmann experimentally studied WAL in various metallic thin films [19] and confirmed that the Maki-Thompson correction gives the most contribution of superconducting fluctuations and cannot be neglected even for temperatures far above T_{c}. Therefore, in our following analysis, both WAL effect and Maki-Thompson term will be taken into account.

Methods

Sample fabrication

The epitaxial aluminum thin film was fabricated on a semi-insulating gallium arsenide (SI-GaAs) substrate in our Varian Gen II MBE system equipped with an arsenic cracking cell. First, a GaAs wafer was heated to 620°C for 20 min for de-oxidation under As flux, and then a 300-nm-thick undoped GaAs buffer layer was deposited at 590°C as the epitaxial template. The sample surface was turned into Ga-rich at 620°C in the absence of As flux. We kept the sample in high vacuum (approximately 3×10^{-10} Torr) until the background As vapor was pumped out. The Al film with an intentional thickness of 3 nm was then deposited at room temperature with a growth rate of 0.366 μm/h.

The 50-μm-wide Hall devices were processed using conventional lithography technique. Al was etched by 2% tetramethylammonium hydroxide (TMAH) for 20 s to transfer the Hall bar pattern from photoresist to our Al film. Ti/Au (30/300 nm) was deposited using e-gun evaporation as the contact electrode. The finished devices were wire-bonded on a ceramic carrier and loaded into ^{4}He cryogenic system equipped with a superconducting magnet. A DC four-terminal electrical measurement has been performed in this work for studying WAL. We have used a Keithley 2602 multi-meter (Keithley Instruments Inc., Cleveland, OH, USA) as a constant current source as well as a voltage meter. Electrical current was set at 3 μA for clear signals and was low enough in order to avoid possible current heating effect. Voltage noise level was at about 5 μV.

Results and discussion

We have used cross-sectional high-resolution transmission electron microscopy (TEM) and atomic force microscopy (AFM) for the investigation of film crystal quality and surface morphology. Figure 1 shows the TEM image of our epitaxial Al film taken with electron beam along the $<0\bar{1}1>_{\mathrm{GaAs}}$ zone axis. A clear interface between the GaAs template and deposited Al can be seen in the middle of the picture. At the bottom of Figure 1, we can see an amorphous layer which may be amorphous carbon from TEM specimen preparation. The thickness of Al layer is about 8 nm which is thicker than the deposited amount because our Al film is percolative as we shall see later in the AFM images. A detailed examination of the TEM image at the interface can show the existence of misfit dislocations, implying that most of the strain in the Al film caused by lattice mismatch between Al and GaAs is released. The inset of Figure 1 is the fast Fourier transform diffraction pattern taken around the interface between GaAs and Al. Clear diffraction spots can be seen. The inner hexagon is the diffraction spots of the bottom GaAs template, and the outer one is for epi-aluminum film, indicating that the epitaxial relationship of Al with GaAs is $(100)_{\mathrm{GaAs}}$ // $(111)_{\mathrm{Al}}$, $<011>_{\mathrm{GaAs}}$ // $<\bar{2}11>_{\mathrm{Al}}$, and $<0\bar{1}1>_{\mathrm{GaAs}}$ // $<0\bar{1}1>_{\mathrm{Al}}$; the last axis is also the observation plane of the TEM image. The axis arrangement is

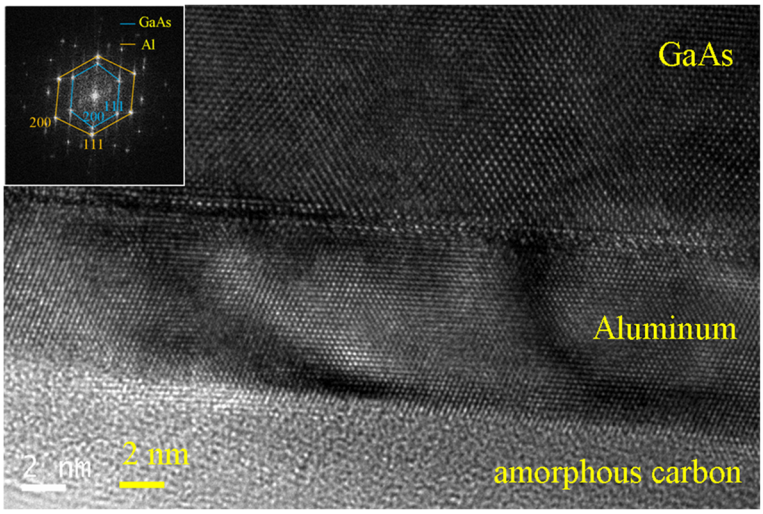

Figure 1 Cross-sectional TEM image of the Al sample. GaAs/Al interface in the middle and the native oxide of Al at the bottom are clearly spotted. The upper left inset is the diffraction pattern showing the GaAs (Al) diffracted spots in the inner (outer) hexagon.

different from the previous works [20-22] probably due to the different surface conditions used. Clear spots indicating good crystal quality and no deformation of the diffraction spots are observed even the strain accumulation due to lattice mismatch could occur in our sample. Figure 2 shows a 1×1 μm^2 AFM image of our Al film. Obviously, a percolating but continuous morphology has been seen. This kind of morphology was generally observed when metal films are deposited onto a semiconductor or dielectric template because of poor affinity between them [23]. Although the bi-polarized atomic bonding of the bottom GaAs template or inhomogeneous surface atomic deformation could

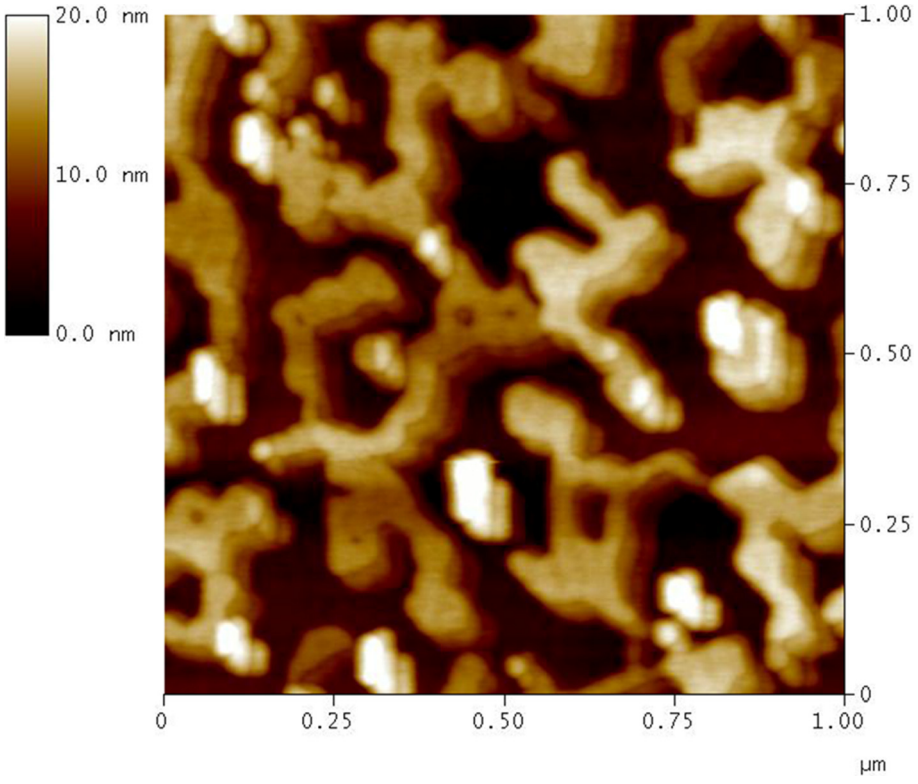

Figure 2 The 1×1 μm^2 AFM image of the Al sample showing the sample roughness is about 4.9 nm.

also play a role here, we have used a smooth Ga-rich surface as the epitaxial template to minimize these two issues. The roughness of the film is about 4.9 nm which is thicker than the deposited thickness and is possibly caused by the Al oxidation after the exposure to the air.

We have measured the sheet resistance R_s of our sample in the temperature range of 1.4 to 10 K. At temperatures higher than 10 K, the signals became noisy and WAL is barely observable. We noted that the Hall resistance R_H is small compared to R_s and remained unchanged even increasing the magnetic field to 1 T. Thus, we neglected the effect of R_H in all the calculation and theoretical fitting. In Figure 3, the measured R_s is plotted against the applied magnetic field at various temperatures, together with the fit to the theoretical model. Around zero magnetic field, clear WAL in our Al film occurs as R_s increases with increasing magnetic fields. In addition, R_s decreases dramatically when the temperature goes below 4.5 K, indicating that the superconducting fluctuation plays an important role here. Therefore, when fitting our data to the theoretical model, we have considered the WAL theory stated in Equation 1 with the first Maki-Thompson term in Equation 2. The later term of Equation 2 vanishes because B_T is always much larger than B_i and B_{so}. The contribution of this term is much less. So, the used fitting formula is given by:

$$\Delta g = \frac{e^2}{\pi h}\left[\frac{3}{2}Y\left(\frac{B_2}{B}\right)-\frac{1}{2}Y\left(\frac{B_i}{B}\right)-\beta Y\left(\frac{B_i}{B}\right)\right]. \quad (3)$$

In our fitting procedure, B_i and β were temperature-dependent fitting parameters. B_{so} was chosen as a temperature-invariant constant because it is commonly accepted that the electron configuration in the half-filled conduction bands is insensitive to the temperature, so the angular momentum and the spin-orbit interaction remains unchanged at all temperature in metals [10-13]. In Figure 3, the solid lines represent theoretic fits of our experimental data at three temperatures as an example. It is clear that the theory can only be applied to small magnetic field. At higher temperatures, the fits can be extended to higher magnetic fields. This is because the Maki-Thompson term is only valid at $B \ll k_B(T - T_c)/4eD$ [15-17].

With the fitted B_i and B_{so}, the inelastic scattering time τ_i and spin-orbit scattering time τ_{so} can be derived by $\tau_i = h/(8\pi eDB_i)$ and $\tau_{so} = h/(8\pi eDB_{so})$, as well as the phase coherent length l_i and spin-orbit interaction length l_{so} by $l_i = (h/8\pi eB_i)^{1/2}$ and $l_{so} = (h/8\pi eB_{so})^{1/2}$. We used Al bulk concentration $n_{Al} = 1.81 \times 10^{29}$ (m^{-3}) to estimate the Fermi velocity ($v_F = 2.03 \times 10^6$ m/s) and Fermi wavelength (λ_F = 0.36 nm) for our sample. Figure 4a shows the extracted parameter $1/\tau_i$ as a function of temperature. The solid horizontal line indicates the level of spin orbit interaction rate $1/\tau_{so}$, and the dashed line represents the theoretic calculation of electron-electron scattering (Nyquist scattering) rate based on the work of Altshuler et al. [24]:

$$\tau_N^{-1} = \frac{e^2 R_s}{2\pi\hbar^2} k_B T \ln\left(\frac{\pi\hbar}{e^2 R_s}\right). \quad (4)$$

In our 3-nm-thick aluminum sample, weak anti-localization changes into weak localization when the

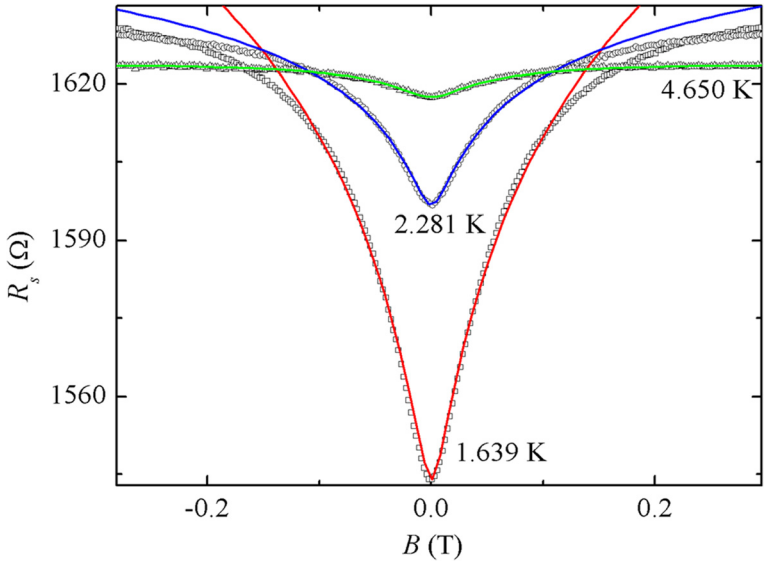

Figure 3 Measured and calculated sheet resistance. Measured (symbols) and calculated (solid lines) sheet resistance as a function of magnetic field of the Al film at 1.639, 2.248, and 4.650 K.

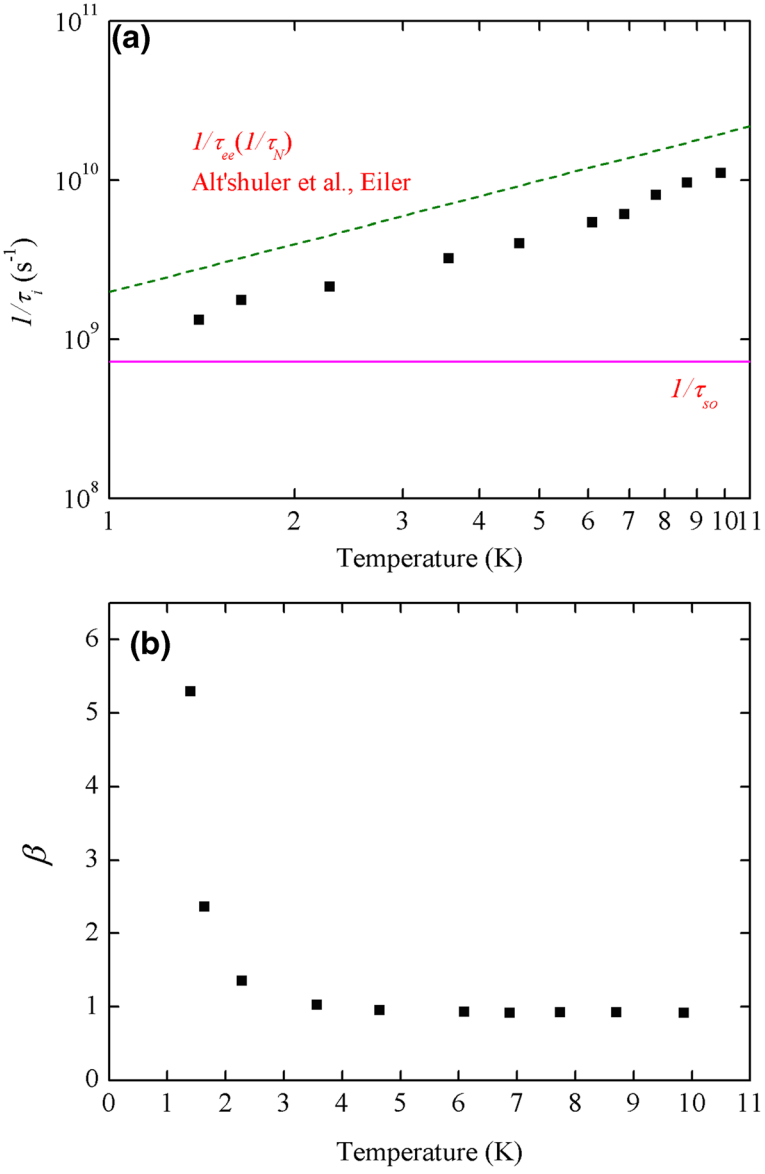

Figure 4 Temperature-dependent dephasing rate and interaction strength. (a) Temperature-dependent dephasing rate ($1/\tau_i$) (symbol) of the Al sample. The horizontal solid line represents the level of spin-orbit interaction rate ($1/\tau_{so}$) and the dashed line represents the theoretic Nyquist scattering rate ($1/\tau_N$). **(b)** Temperature dependence of the interaction strength β.

temperature goes above 10 K. In the temperature range for existing WAL ($T < 10$ K), we found that $1/\tau_i$ is proportional to T, which agrees with the theoretic prediction of Nyquist scattering (dashed line) in the same order.

We would like to emphasize that our ultrathin Al film has a very high carrier concentration ($n \sim 10^{29}$ m^{-3}), so it is actually in mixed dimensions. That is, considering the density of states and diffusive motion, it is treated as a 3D system because the film thickness d is much larger than the Fermi wavelength λ_F ($d \gg \lambda_F \sim 10^{-1}$ nm) and its mean free path of electrons l_0 ($d \gg l_0 \sim 10^{-1}$ nm in our sample). However, in terms of electron dephasing, the film thickness is much less than the dephasing length l_i ($d \ll l_i \sim$ few tens of nanometers) so the system is two-dimensional. Previous experimental studies on clean and dirty Al thin films demonstrated that, only for the temperature near T_c, Nyquist scattering was the major dephasing mechanism. When the temperatures were higher than about 4 K, electron-phonon scattering dominated the dephasing process [9-14]. In contrast, our results show a pure electron-electron dephasing all the way up 10 K. For a type I superconducting material, there is only one experimental result on clean titanium film exhibiting a full T^{-1} dependence of dephasing rate

[25]. However, our sample is in the dirty limit as the sheet resistivity of our sample is over 1.6 kΩ, at least one order higher than those all of their samples. On the other hand, for type II superconductors such as ZrRh and TaN, most experimental works did not observe the pure T^{-1} dependence of dephasing rate [26,27]. It is worth mentioning that the observation of Giannouri et al. [28] with their NbTa film is very similar to ours except that the sudden drop of dephasing rate at temperature approaching T_c has not been seen even at 1.4 K in our experiment.

Dephasing process which purely comes from electron-electron scattering observed here is unusual but is relatively easy to be obtained in semiconductor-based 2D systems, such as 2D electron or hole gases (2DEG and 2DHG), formed by modulation-doped heterostructures. The carriers (electrons or holes) are confined by the triangular potential well caused by remote ionized dopants and limited in the few monolayers next to the heterostructure interface. The carrier concentration of 2DEG or 2DHG is controlled in the range of $10^{10} \sim 10^{12}$ cm^{-2}, so the Fermi wavelength λ_F easily exceeds the size of the confinement potential well and the system is quantized in this dimension to become two-dimensional. However, for metallic materials even down to a few nanometers, the carrier concentration is still as high as 10^{15} cm^{-2}, which makes the λ_F is much smaller than its thickness. Recently, the experimental results of WAL in various semiconductor heterostructures were published, including AlGaN/GaN, GaAs/InGaAs, InP/InGaAs, and AlGaAs/GaAs [29-35]. Most of these works demonstrated a full T^{-1} dependence of the dephasing rate up to 10 K and considered as consistent with the theoretic calculation of Nyquist scattering because of their 2D nature. In our Al film, the observed pure 2D-like dephasing indicates that the superconducting metallic film can be an ideal 2D system in inelastic process.

We wish to address the issue of zero-temperature saturation rate ($1/\tau_i^0$) that is the dephasing rate in the zero temperature limit. The origin of the saturation rate is still under debate for the time being [36]. Some of the reported experimental works on superconducting metallic materials revealed a divergence dephasing rate when the temperature approached T_c [9,10,13,26,27]. In contrast, such situations have not been observed in our sample that exhibits a full Nyquist scattering rate from liquid helium temperatures to 10 K, thus could be helpful for developing the related theory.

In Figure 4b, the electron-electron interaction strength parameter β in the Maki-Thompson correction term is plotted as a function of temperature. It is clear that β has a trend to diverge at temperature approaching T_c, as expected with Larkin's theory [18]. The value of our sample decreases dramatically with the increasing temperature because the superconducting effect becomes less significant. It is noted that β does not vanish but converge to about 0.9 instead. A similar result was observed in ZrRh films [26]. Further investigations on this non-zero β are certainly needed.

We note that the sheet resistivity of our sample is about 1.6 kΩ. The mean free path l_0 actually is 0.082 nm estimated by the Drude model, which is slight shorter than λ_F. This appears to contradict to the basic assumption of the WAL theory that WAL occurs in a weakly disordered system ($l_0 \gg \lambda_F$). In a strongly disordered system, WAL should not be observed. We believe that, due to the percolative morphology of our sample, the actual electron path is much longer than the Hall bar size; therefore, the mean free path l_0 has been underestimated.

Similar to the WAL effect, the universal conductance fluctuations (UCFs) due to the electron (or hole) interference between two classical paths is closely related to the phase coherent length l_i [37-40]. We have also examined the conductance fluctuations in our measured data, but no clear UCFs are observed, which could be due to the large size of our device and the limit of the measurement system noise (approximately 5 μV).

Conclusions

We have presented the structural and electrical characterization of the ultrathin percolating aluminum film grown by MBE. The TEM results indicate a superior crystal quality of the epitaxial aluminum film. WAL revealed by low-temperature magnetoresistance measurement showed its unusual dephasing mechanism. At all temperatures that WAL exists, a pure electron-electron scattering was observed, so the aluminum film behaves as an ideal two-dimensional system in this aspect. Based on this, we conclude that the MBE-grown aluminum films could achieve the two-dimensional limit of a superconducting metallic material.

Competing interests

The authors declare that they have no competing interests.

Authors' contributions

S-WL carried out the sample growth, electrical measurements, and data analysis and drafted the manuscript. Y-HW and LC performed the TEM sample preparation and characterization. LC, C-TL, and S-DL participated in the data analysis and model discussion and helped to draft the manuscript. All authors read and approved the final manuscript.

Acknowledgements

We thank the financial support from the NSC and ATU program of MOE in Taiwan. The equipment help from the Center for Nano Science and Technology at the National Chiao Tung University and National Device Laboratory is highly appreciated. C-TL acknowledges the support from the MOST, Taiwan (grant numbers: MOST 103-2918-I-002-028 and MOST 102-2119-M-002-016-MY3).

Author details

[1]Department of Electronics Engineering, National Chiao Tung University, 1001 University Road, Hsinchu 30010, Taiwan. [2]Department of Materials

Science and Engineering, National Chiao Tung University, Hsinchu 30010, Taiwan. [3]Department of Physics, National Taiwan University, Taipei 10617, Taiwan. [4]Geballe Laboratory for Advanced Materials (GLAM), Stanford University, Stanford, CA 94305, USA.

Received: 12 December 2014 Accepted: 24 January 2015
Published online: 18 February 2015

References

1. Hikami S, Larkin AI, Nagaoka Y. Spin-orbit interaction and magnetoresistance in two-dimensional random system. Prog Theor Phys. 1980;63:707.
2. Baker AMR, Alexander-Webber JA, Altebaeumer T, Janssen TJBM, Tzalenchuk A, Lara-Avila S, et al. Weak localization scattering lengths in epitaxial, and CVD graphene. Phys Rev B. 2012;86:235441.
3. Steiberg H, Laloë J-B, Fatemi V, Moodera JS, Jarillo-Herrero P. Electrically tunable surface-to-bulk coherent coupling in topological insulator thin films. Phys Rev B. 2011;84:233101.
4. Lang M, He L, Kou X, Upadhyaya P, Fan Y, Chu H, et al. Competing weak localization and weak antilocalization in ultrathin topological insulators. Nano Lett. 2013;13:48.
5. Neumaier D, Wagner K, Geißler S, Wurstbauer U, Sadowski J, Wegscheider W, et al. Weak localization in ferromagnetic (Ga, Mn)As nanostructures. Phys Rev Lett. 2007;99:116803.
6. Kallaher RL, Heremans JJ. Spin and phase coherence measured by antilocalization in n-InSb thin films. Phys Rev B. 2009;79:075322.
7. Kallaher RL, Heremans JJ, Goel N, Chung SJ, Santos MB. Spin-orbit interaction determined by antilocalization in an InSb quantum well. Phys Rev B. 2010;81:075303.
8. Ebisawa H, Maekawa S, Fukuwama H. Pair breaking parameter of two-dimensional dirty superconductors. Solid State Commun. 1983;45:75.
9. Gordon JM, Lobb CJ, Tinkham M. Divergent phase-breaking rate in aluminum films from magnetoresistance measurements. Phys Rev B. 1984;29:5232.
10. Gordon JM, Goldman AM. Electron inelastic scattering in aluminum films and wires at temperatures near the superconducting transition. Phys Rev B. 1986;34:1500.
11. Shinozaki B, Kawaguti T, Fujimori Y. Magnetoresistance near superconducting transition temperature of aluminum films. J Phys Soc Jpn. 1986;55:2364.
12. Santhanam P, Prober DE. Inelastic electron scattering mechanisms in clean aluminum films. Phys Rev B. 1984;29:3733.
13. Shinozaki B, Kawaguti T, Fujimori Y. Localization and interaction effects in weakly localized region in aluminum films. J Phys Soc Jpn. 1984;53:3303.
14. Santhanam P, Wind S, Prober DE. Localization, superconducting fluctuations, and superconductivity in thin films and narrow wires of aluminum. Phys Rev B. 1987;35:3188.
15. Maki K. Critical fluctuation of the order parameter in a superconductor. I Prog Theor Phys. 1968;40:193.
16. Thompson RS. Microwave, flux flow, and fluctuation resistance of dirty type-II superconductors. Phys Rev B. 1970;1:327.
17. Santos JMBLd, Abrahams E. Superconducting fluctuation conductivity in a magnetic field in two dimensions. Phys Rev B. 1985;31:172.
18. Larkin AI. Reluctance of two-dimensional systems. JETP Lett. 1980;31:219.
19. Bergmann G. Quantum corrections to the resistance in two-dimensional disordered superconductors above T_c: Al, Sn, and amorphous $Bi_{0.9}Tl_{0.1}$ films. Phys Rev B. 1984;29:6114.
20. Cho AY, Dernier PD. Single-crystal-aluminum Schottky-barrier diodes prepared by molecular-beam epitaxy (MBE) on GaAs. J Appl Phys. 1978;49:3328.
21. Ludeke R, Chang LL, Esaki L. Molecular beam epitaxy of alternating metal-semiconductor films. Appl Phys Lett. 1973;23:201.
22. Lin S-W, Wu J-Y, Lin S-D, Lo M-C, Lin M-H, Liang C-T. Characterization of single-crystalline aluminum thin film on (100) GaAs substrate. Jpn J Appl Phys. 2013;52:045801.
23. Ruffino F, Grimaldi MG. Island-to-percolation transition during the room-temperature growth of sputtered nanoscale Pd films on hexagonal SiC. J Appl Phys. 2010;107:074301.
24. Altshuler BL, Aronov AG, Khmelnitsky DE. Effects of electron-electron collisions with small energy transfers on quantum localization. J Phys C: Solid State Phys. 1982;15:7367.
25. Vangrunderbeek J, Van Haesendonck C, Bruynseraede Y. Electron localization and superconducting fluctuations in quasi-two-dimensional Ti films. Phys Rev B. 1989;40:7594.
26. Giannouri M, Rocofyllou E, Papastaikoudis C, Schilling W. Weak-localization, Aslamazov-Larkin, and Maki-Thompson superconducting fluctuation effects in disordered $Zr_{1-x}Rh_x$ films above T_c. Phys Rev B. 1997;56:6148.
27. Breznay NP, Kapitulnik A. Observation of the ghost critical field for superconducting fluctuations in a disordered TaN thin film. Phys Rev B. 2013;88:104510.
28. Giannouri M, Papastaikoudis C, Rosenbaum R. Low-temperature transport properties of $Nb_{1-x}Ta_x$ thin films. Phys Rev B. 1999;59:4463.
29. Lu J, Shen B, Tang N, Chen DJ, Zhao H, Liu DW, et al. Weak anti-localization of the two-dimensional electron gas in modulation-doped $Al_xGa_{1-x}N$/GaN heterostructures with two subbands occupation. Appl Phys Lett. 2004;85:3125.
30. Thillosen N, Schäpers T, Kaluza N, Hardtdegen H, Guzenko VA. Weak antilocalization in a polarization-doped $Al_xGa_{1-x}N$/GaN heterostructure with single subband occupation. Appl Phys Lett. 2006;88:022111.
31. Thillosen N, Cabañas S, Kaluza N, Guzenko VA, Hardtdegen H, Schäpers T. Weak antilocalization in gate-controlled $Al_{1-x}Ga_xN$/GaN two-dimensional electron gases. Phys Rev B. 2006;73:241311(R).
32. Minkov GM, Sherstobitov AA, Germanenko AV, Rut OE, Larionova VA, Zvonkov BN. Antilocalization and spin-orbit coupling in the hole gas in strained GaAs/$In_xGa_{1-x}As$/GaAs quantum well heterostructures. Phys Rev B. 2005;71:165312.
33. Minkov GM, Germanenko AV, Rut OE, Sherstobitov AA, Golub LE, Zvonkov BN, et al. Weak antilocalization in quantum wells in tilted magnetic fields. Phys Rev B. 2004;70:155323.
34. Studenikin SA, Coleridge PT, Ahmed N, Poole PJ, Sachrajda A. Experimental study of weak antilocalization effects in a high-mobility $In_xGa_{1-x}As$/InP quantum well. Phys Rev B. 2003;68:035317.
35. Millo O, Klepper SJ, Keller MW, Prober DE, Xiong S, Stone AD, et al. Reduction of the mesoscopic conductance-fluctuation amplitude in GaAs/AlGaAs heterojunctions due to spin-orbit scattering. Phys Rev Lett. 1990;65:1494.
36. Lin JJ, Bird JP. Recent experimental studies of electron dephasing in metal and semiconductor mesoscopic structures. J Phys: Condens Matter. 2002;14:R501.
37. Lee PA, Stone AD, Fukuyama H. Universal conductance fluctuations in metals: effects of finite temperature, interactions, and magnetic field. Phys Rev B. 1987;35:1039.
38. Li Z, Chen T, Pan H, Song F, Wang B, Han J, et al. Two-dimensional universal conductance fluctuations and the electron-phonon interaction of surface states in Bi_2Te_2Se microflakes. Sci Rep. 2012;2:595.
39. Kahnoj SS, Touski SB, Pourfath M. The effect of electron-electron interaction induced dephasing on electronic transport in graphene nanoribbons. Appl Phys Lett. 2014;105:103502.
40. Weber B, Ryu H, Matthias Tan Y-H, Kilmeck G, Simmons MY. Limits to metallic conduction in atomic-scale quasi-one-dimensional silicon wires. Phys Rev Lett. 2014;113:246802.